Finite element-based framework to study the response of bituminous concrete pavements under different conditions

Kumar, Abhinav; Gupta, Ankit; Anupam, Kumar; Wagh, Vivek Pratap

DOI
10.1016/j.conbuildmat.2024.135368

Publication date
2024

Document Version
Final published version

Published in
Construction and Building Materials

Citation (APA)
Kumar, A., Gupta, A., Anupam, K., & Wagh, V. P. (2024). Finite element-based framework to study the response of bituminous concrete pavements under different conditions. *Construction and Building Materials*, *417*, Article 135368. https://doi.org/10.1016/j.conbuildmat.2024.135368

Construction and Building Materials 417 (2024) 135368

Contents lists available at ScienceDirect

Construction and Building Materials

journal homepage: www.elsevier.com/locate/conbuildmat

Finite element-based framework to study the response of bituminous concrete pavements under different conditions

Abhinav Kumar [a], Ankit Gupta [a], Kumar Anupam [b,*], Vivek Pratap Wagh [a]

[a] Department of Civil Engineering, IIT BHU, Varanasi, India
[b] Department of Civil Engineering & Geoscience, Delft University of Technology, Delft, the Netherlands

ARTICLE INFO

Keywords:
Effect of air voids
Indian traffic conditions
Generalised Kelvin model
Creep compliance
Resilient modulus

ABSTRACT

In most of developing countries across the world, pavement design is still based on an empirical approach that may result in premature failure or overdesigned pavements. A shift from an empirical to a semi-mechanistic or mechanistic approach is the need of modern time. In this regard, computational tools such as finite element (FE) are being successfully utilized to gain deeper insights because such tools have allowed researchers to study the complex behaviour of bituminous concrete (BC) materials. It is well recognized that BC material typically exhibits viscoelastic/visco-elasto-plastic behaviour depending on applied loading (including temperature) conditions. However, due to the complexity of the whole procedure yet many pavement design tools consider them as pure elastic material. The aim of this research is to develop FEM based simple and practical framework to evaluate the structural response of BC material with viscoelastic material characterization which can be an effective tool to predict field behaviour with commonly available pavement material tests. Such a framework will be helpful in analysing variations in the critical response of BC pavement with varied traffic loads and ambient temperatures. The framework provides a relatively simple procedure to obtain the viscoelastic parameters of BC mix with a creep compliance test conducted at different temperatures. It was concluded that Creep compliance data if pre-smoothened by the Power law model reduces mathematical optimization issues to some extent. Furthermore, with the obtained parameters, a 3-dimensional FE model was developed to obtain sensitivity to critical stresses, strains, and vertical deformations at desired conditions. Material characterization of unbound granular layers was evaluated through resilient modulus based on empirical relations. Analysis was carried out taking into consideration the traffic load, contact pressure, mix type, air-void, and temperature variation.

1. Introduction

Direct/indirect empirical approaches in the current pavement design procedures may result in premature pavement failure or over-designed pavements [1]. However, these empirical approaches are still being practiced in many developing countries around the world. In modern days, a lot of developing countries such as India are identifying an urgent need to shift their design practices from empirical to semi-mechanistic/mechanistic pavement design suited to their local requirements. In such cases, different material characterization tests will be required. One of the important aspects that need to be incorporated is the time and temperature dependency of the pavement materials. Whereas, for the characterization of time/temperature dependency of binding materials, Dynamic shear rheometer (DSR) tests are often used, however, for mixtures either no such tests are carried out or they are scarcely used. In the authors' opinion, the characterization of temperature dependency of the mixture is important for countries like India where huge temperature variation across the region and seasons is observed.

In India, bituminous concrete (BC) pavements which are multilayer structures with different material properties [2] are becoming popular [3]. Depending on the aggregate gradations, the Ministry of Road Transport & Highways [4], India has categorised BC as BC-1 and BC-2. The nominal aggregate size of BC-1 is 19 mm whereas that of BC-2 is 13.2 mm. BC-2 is composed of a higher percentage of fine aggregates (62% aggregates passing 4.75 mm IS sieve) than BC-1 (50% aggregates passing 4.75 IS sieve). So, the minimum binder content specified by [4] for BC-2 is higher (5.4%) than BC-1 (5.2%). Since BC-2 consists of a higher percentage of fine aggregates, the prepared mix provides a smoother surface than BC-1, which helps in fixing deformation

* Corresponding author.
E-mail address: k.anupam@tudelft.nl (K. Anupam).

https://doi.org/10.1016/j.conbuildmat.2024.135368
Received 28 August 2023; Received in revised form 1 January 2024; Accepted 6 February 2024
Available online 13 February 2024

measuring transducers and motivated to consider in the present study as the top layer. Depending on material choices and their production processes, they exhibit different mechanical characteristics resulting in different performances.

As discussed in the previous paragraph, understanding the mix behaviour is important for reaching the expected lifetime. Therefore, uncertainties related to the mix design phase will result in a significant reduction in its lifetime. To minimise such risks, road agencies in India mandate the testing of these mix samples under controlled laboratory conditions, for example, the Marshall stability test, resilient modulus test, etc. However, tests measuring the viscoelastic characterization of the mixture are not posed as a requirement. It is well known that depending upon loading and ambient (temperature) conditions, asphaltic materials such as BC can exhibit viscoelastic/visco-elasto-plastic behaviour [5]. Hence, many researchers in the past have studied the viscoelastic behaviour of binder [6,7] and bituminous mixes [8–13] for the analysis of flexible pavement. It is important to measure the properties of BC at a wide range of frequencies and temperatures to obtain viscoelastic behaviour. At high temperatures or under slow-moving loads, it may exhibit a purely viscous flow reflecting its propensity towards rutting. However, at relatively low temperatures and fast-moving loads, it becomes progressively harder and eventually brittle, which makes it vulnerable to non-load-associated distresses like low-temperature cracking. Moreover, it is susceptible to fatigue-related problems at normal temperatures as most of the vehicular load is applied at these temperatures [14].

The characterization of viscoelastic properties is often done by measuring creep behaviour [15]. The creep-related tests are popular because these tests make it possible to determine and separate the time-independent (elastic strain) and time-dependent (viscoelastic) components of the strain response [16] in a simplified way. In addition, parameters obtained from creep tests at low temperatures (m-value) are used to predict thermal cracking development and propagation, and those at high temperatures are used to predict rutting in the HMA [17]. Once creep compliance is obtained, viscoelastic behaviour is obtained through the time-temperature superposition principle [15].

Even though, as highlighted in the previous section, viscoelastic characteristics are important to be included in the design of pavements, most of the present mechanistic design standards [10,18–20] assume the BC layer as elastic during multilayer pavement analysis. Some of the modern-day tools (ABAQUS, ANSYS, 3-D Move) allow for the inclusion of viscoelastic characteristics for pavement design. However, in India, generally, elastic modulus (E) and Poisson ratio (υ) are used to characterize materials as linear elastic and subsequently used as input parameters in different design tools [21]. However, researchers [22] concluded that the elastic theory cannot represent permanent deformation or delayed recovery, which is an important characteristic of BC materials. BC shows elastic behaviour at low temperatures only and thus the use of elastic theory to explain material's response is limited to low-temperature analysis [23]. For intermediate and high temperatures, elastic theory often underestimates these responses [23].

As explained in the previous paragraph, since BC exhibits viscoelastic behaviour, controlling and conducting experiments for all different types of combinations to represent field conditions is nearly impossible. In such cases, analytical and computational tools are readily used. Increasing computational capabilities have allowed pavement scientists to study complex material behaviour using tools like finite element (FE), discrete element (DE), etc. [5]. To include viscoelastic characteristics in such tools, often a generalised Kelvin viscoelastic model (GKM) or Prony series model [22,24] is used. Furthermore, Zhang et al. [25] showed that the generalized Maxwell model is well suited for the prediction of bituminous concrete deformation under repeated load.

State-of-the-art equipment such as dynamic modulus test, bending beam rheometer test, and creep compliance test is recommended to be used in developed nations. However, in developing nations, often limited resources are available and therefore conducting different types of tests is not always possible. In such cases, a simple test is required to obtain the desired behaviour. Creep compliance test facility is readily available in most of the research institutions in India. Creep compliance test measures material deformation with time at different temperatures which is defined as time-dependent strain per unit stress [26]. In addition to temperature, creep compliance varies with the constituent's properties and their proportion in the bituminous mix. Compacted mix properties like air void also affect creep compliance results, hence, affecting GKM parameters. Since India is a region with a tropical climate and temperature varies from − 2° to 42° C throughout the year, it is important to study mix behaviour at different temperatures. Also, the lack of quality control in mix compaction results in a wide range of air voids. Under these conditions, a lot of uncertainties in the calculation of GKM are expected depending upon region and season. At the end, these uncertainties will result in unreliable design and a significant reduction in their expected lifetime. This article aims to study some of these effects for designing a pavement with BC-2 materials as surface course including their viscoelastic characteristics.

In this study, material properties of various layers were characterized to evaluate the structural response of typical pavements. Material characterization of unbound granular layers is based on resilient modulus and Poisson's ratio as recommended by IRC:37 in India. A continuum-based finite layer approach, 3-D Move [27], has been used in this study as a reference tool to predict and validate the structural response of BC pavement. it can identify the elastic and viscoelastic moduli of BC pavement [28]. A 3-dimensional FE model of BC pavement has been created in ABAQUS (FE-based analysis tool). The present study uses ABAQUS for predicting the sensitivity of the structural response of bituminous concrete pavement at various air voids in BC-2 mix, temperature, tire load, and contact pressure.

1.1. Framework of the paper

For easy understanding and quick review, the manuscript has been arranged into different sections and subsections. The first section provides various literature available on the viscoelastic material characterization of bituminous concrete, pavement modelling, structural response prediction, the objective of the study, and the methodology adopted. The second section presents lab test results of the physical properties of materials used in BC-2, mix design, and creep compliance test method. The third section discusses how creep compliance data has been fitted to the generalised Kelvin model. Evaluation of Prony series constants and conversion of creep compliance data to relaxation modulus has also been discussed. Material characterization of unbound granular layers has been discussed as per the guidelines of IRC:37–2018 in the last part of this section. The fourth section presents finite element modelling of bituminous concrete pavement, boundary conditions, and pavement structure. The fifth section discusses the results of the creep compliance test, structural response of the pavement, and statistical analysis using 2-way ANOVA for understanding the significance of contact pressure and tire load on pavement response. The sixth and seventh sections provide the critical conclusion and future scope of the study respectively.

1.2. Objective and scope

The objective of this paper is to predict the sensitivity of the structural response of bituminous concrete pavement subjected to various load classes, contact pressure, air void in BC mix, and temperature for Indian roads. A constitutive framework for evaluating Prony series parameters of the BC-2 mix for Indian conditions has been discussed. Test temperature has been selected corresponding to average temperature variation in summer and winter in India. Tire load has been selected which corresponds to light to heavy vehicular load passes on Indian roads.

For linear viscoelastic material characterization of bituminous

concrete, a creep compliance test has been employed for the determination of creep compliance as a function of axial deformation in the mix with time. Since the present study aims to evaluate the influence of air voids on the creep behaviour and relaxation modulus, the compaction efforts were varied at optimum binder content (OBC) to obtain different air voids in compacted Marshall specimens. The present study employs a dynamic testing system for the experimental determination of creep compliance. For modelling the viscoelastic properties of BC-2, a generalized Kelvin model has been used.

For characterizing materials used in unbound granular layers, the resilient modulus and Poisson's ratio have been used considering the elastic response of materials as suggested by IRC:37–2018 [29], code of practice for the design of flexible pavement in India. Resilient modulus has been evaluated using empirical relations based on CBR values of supporting layers.

A 3-dimensional bituminous concrete pavement has been modelled in ABAQUS (FE-based software) to identify the response to material properties of the bituminous mix. The analysis was carried out at three different contact pressures of 420, 560, and 740 kPa and three different single-wheel loads of 20, 25, and 30 kN. The effect of air void, temperature, tire load, and contact pressure on bituminous concrete pavement response in terms of normal compressive stress (σ_z), and normal compressive strain (ε_z) has been noted and discussed.

2. Materials

Locally available silty sand has been used as subgrade material. The free swelling index was found 12% which is within the specified limit of a maximum of 50% by IS:2720-part 40 [30]. Maximum dry unit weight when tested as per IS:2720-part 8 was found to be 17.91 kN/m^3 which is higher than the minimum specified value of 17.5 kN/m^3. The physical requirements of aggregates to be used in the granular subbase and base layer and binder for the BC layer have been discussed in the next subsections.

2.1. Aggregate

In the present study, Calcareous aggregate (Dolomite) was used to prepare bituminous mixtures. These are common types of aggregate used for the construction of flexible pavement in India. It is basic in nature and provides good bonding with bitumen compared to acidic aggregates [31]. To check the quality of aggregates, the following test was conducted as per MoRTH [4] specifications followed in India as shown in Table 1.

2.2. Asphalt binder

A viscosity-graded binder, VG30 was used. This is the most common binder type used in road construction in India. Physical tests were performed on the binder in accordance with IS 73:2013 and ASTM standards [34], as shown in Table 2. In India, binder gradation is based on viscosity so test protocol and specifications for high-temperature continuous grade and performance grading are not available. High-temperature continuous grade and performance grade tests using a dynamic shear rheometer were conducted in accordance with ASTM D6373. Table 2 presents some of the physical properties of the asphalt binder, the test protocol used for their evaluation, and the limits in which these results should fall to be used as a bituminous mix binding material.

Table 1
Physical properties of aggregate.

Properties	Combined flakiness and elongation index	Los Angeles abrasion value	Aggregate impact value
Specification limit	Max 35%	Max 40%	Max 30%
Methodology	IS 2386-Part I[32]	IS 2386-Part IV [33]	IS 2386-Part IV [33]
Value obtained	18%	20%	16.7%

Table 2
Physical properties of asphalt binder.

Properties	Value obtained	Methodology	Specification limit
Penetration value at 25° C, 0.1 mm	60	IS 1203[35]	Min 45
Absolute viscosity at 60° C, Poises	2900	IS 1206-Part 2 [36]	2400-3600
Softening point, °C	51.5	IS 1205[37]	Min 47
High-temperature continuous grade (°C)	65.1	ASTM D6373	-
High-temperature PG (°C)	PG64-XX	ASTM D6373	-

2.3. Mix design

The bituminous concrete (BC-2) gradation in accordance with the Ministry of Road Transport and Highways, India [4] with a nominal maximum size of aggregate of 13.2 mm was used for the preparation of the bituminous mixture. The obtained gradation and specification limits are shown in Fig. 1. In India, all the design and mix performance tests are based on Marshall mix samples. So, in this study, the Marshall mix design was carried out in accordance with the Asphalt Institute specification, MS-2 [38]. The OBC was evaluated for samples prepared using VG 30.

Table 3 shows the volumetric properties of Marshall mix samples for BC-2 gradation with VG30 asphalt binder. The compaction efforts required to achieve particular air voids were determined from the relationship between air voids and compaction by interpolation method.

2.4. Creep compliance test

The test sample was prepared with all the volumetrics as discussed in Section 2.3 (see Table 3). Creep compliance test procedures apply to samples having a maximum aggregate size of 38 mm or less. As per AASHTO T-322, the sample should be 38 to 50 mm high and 150 ± 9 mm in diameter. Both ends of the sample were cut by 6 mm to provide smooth and parallel surfaces for better mounting of the deformation measurement transducer (LVDT). Four brass gauge points were attached to each flat face of the sample. The gauge distance was kept at 50 mm. Two 0.1 mm LVDTs were connected on each face, one in the axial direction of loading and the other in the lateral direction. The specimen was allowed to remain at test temperature for 3 h prior to testing for conditioning of the sample. A constant load of 2 kN for 100 s was applied on the diametrical axis of the sample. Creep load was selected to keep the strain within the linear viscoelastic range i.e., produces a horizontal deformation of 0.00125 mm to 0.0190 mm. Based on horizontal and vertical deformations, normalised deformations and trimmed mean were calculated as per AASHTO T-322 for evaluating the creep compliance of the mix. The test setup for creep compliance is shown in Fig. 2.

3. Material modelling

3.1. Material characterization of bituminous concrete

The generalized Kelvin model (GKM) and the generalized Maxwell model (GMM) are the two widely used models for characterizing linear viscoelastic properties of bituminous mix [39]. These models best fit the relaxation modulus and creep compliance as a series of decaying exponentials also called as Dirichlet or Prony series [39]. Viscoelastic

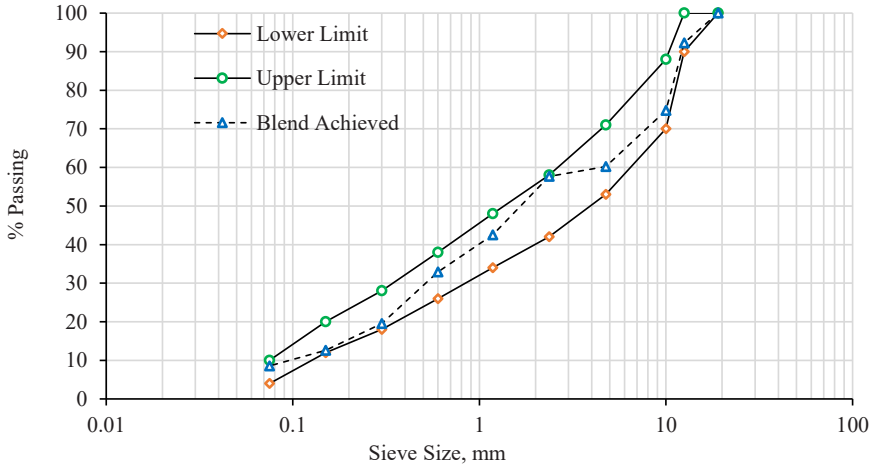

Fig. 1. Aggregate gradation adopted in the study.

Table 3
Summary of volumetric properties of Marshall mix sample.

Binder type	OBC (%)	G_{mb}	G_{mm}	Air void (%)	VMA (%)	VFB (%)	Stability (kN)	Flow (mm)
VG 30	5.8	2.400	2.501	4.038	13.1	71	18.8	3.8
Specification limit	Min 5.4	-	-	3 - 5	Min 12	65 - 75	> 9	2 - 4

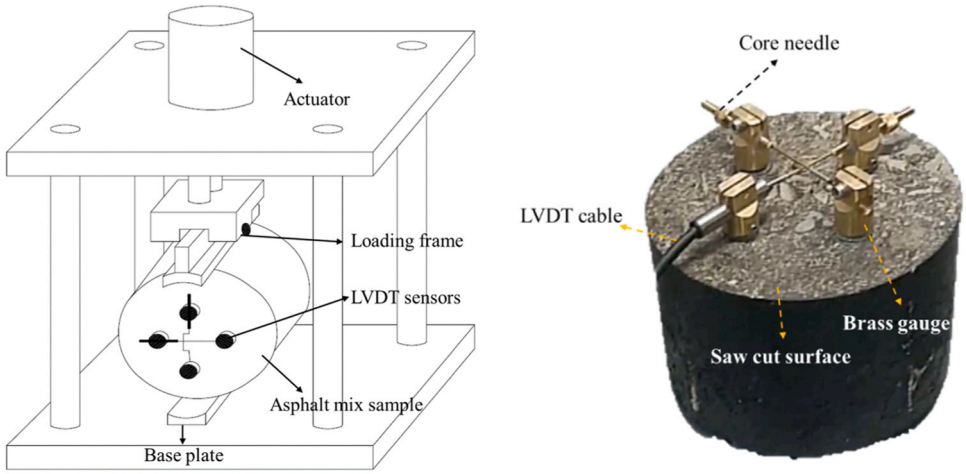

Fig. 2. (a) Specimen loading frame (AASHTO T-322) (b) BC-2 sample and deformation measurement transducers.

functions represented using the Prony series can be mathematically converted from the time domain to the frequency domain [39]. The GMM for a viscoelastic solid consists of a spring and several Maxwell elements assembled in parallel. Maxwell elements are a combination of spring and dashpot representing elastic and viscous components of the mix. The GMM is convenient for analysing the relaxation behaviour of linear viscoelastic materials. The relaxation modulus of GMM has the form of the Prony series as shown below:

$$E(t) = E_{\infty} + \sum_{k=1}^{n} E_k \exp\left(-\frac{t}{\rho_k}\right) \tag{1}$$

Where E_{∞} is the equilibrium modulus, ρ_k, and E_k are the relaxation time and the stiffness of the kth Maxwell element respectively. The complex modulus of GMM in the frequency domain is given by Eq. 2 [40].

$$E^*(\omega) = E_{\infty} + \sum_{k=1}^{n} \frac{i\omega\rho_k E_k}{1 + i\omega\rho_k} \tag{2}$$

where ω is the angular frequency. However, the GKM consisting of a spring and several Voigt elements connected in series is convenient for analysing the creep behaviour of viscoelastic material [39]. The complex compliance (D*) and creep compliance (D(t)) of GKM is given by [40] as follows:

$$D^*(\omega) = D_o + \sum_{k=1}^{n} \frac{D_k}{1 + i\omega\tau_k} \tag{3}$$

$$D(t) = D_o + \sum_{k=1}^{n} D_k\left[1 - \exp\left(-\frac{t}{\tau_k}\right)\right] \tag{4}$$

where D_o is instantaneous creep compliance, τ_k, and D_k are the retardation time and creep compliance of the kth Voigt element respectively. Model parameters τ_k and D_k are determined by a series of constraint optimization processes using the least square approach [41].

In this study, the Prony series and power law series have been used to model linear viscoelastic material properties of BC-2. Power law series is a simple power function of time in which evaluation of only instantaneous creep compliance and time exponent is required [42]. A power law model if used with multiple power law terms can present a smooth and reliable viscoelastic response of bituminous mix with minimal impact from local variance in data. However, from the computational point of view, a Prony series representation is preferable to a power law model because of its efficiency and better exponential fitting of material response [43]. In the present study, the five-term Prony series and single-term Power series are used to model the viscoelastic properties of BC-2. It is noted that the Power Law series has been kept simple just for the pre-smoothing and comparison purposes (see Eq. 5). Pavement response analysis has been carried out based on outcomes of the Prony series model only.

$$D(t) = D_o + D_1(t)^n \tag{5}$$

where D_o is instantaneous creep compliance, D_1 is the model parameter and n is the time exponent. In both models, the square of the error between the experimental creep compliance value and model predicted value is minimized to evaluate model constants [41].

The Prony series model was also used to convert creep compliance to relaxation modulus E(t). The interconversion technique is based on an approximate solution developed by Schapery and Park [44]. The relaxation modulus and creep compliance are related by a convolution integral, as follows:

$$\int_0^t E(t-\tau)D(\tau)d\tau = t \quad for \quad t > 0 \tag{6}$$

A common method for the numerical solution requires the decomposition of the integral into several intervals as the spread of the function may extend to a few decades [43]. However, this may render inaccurate results and cause computational difficulties if intervals are not carefully selected [43]. Therefore, another approach [44] in which data within each small interval are locally fitted to the pure power law model has been used. The relaxation modulus within one interval was predicted using the following equation as proposed by [44]:

$$E(t) = \frac{\sin(n\pi)}{n\pi D(t)} \tag{7}$$

where n is the time exponent of local power law expression.

3.2. Material characterization of unbound granular layers

The material properties of unbound granular layers were obtained using empirical relations as provided by IRC:37–2018 [29]. These relations are based on the CBR value of subgrade soil and are given by:

$$M_{RS} = 10 \times CBR \quad for \quad CBR \leq 5\% \tag{8}$$

$$M_{RS} = 17.6 \times (CBR)^{0.64} \quad for \quad CBR > 5\% \tag{9}$$

where M_{RS} is the resilient modulus of subgrade soil (MPa), and CBR is California bearing ratio of subgrade soil (%). The granular base and granular subbase layer are considered as a single layer for the analysis; therefore, a single modulus value is assigned to the combined layer. the resilient modulus of the granular layer from its combined thickness and modulus of the supporting layer is estimated as:

$$M_{R(granular)} = 0.2(h)^{0.45} \times M_{R(support)} \tag{10}$$

where $M_{R(granular)}$ is the resilient modulus of the granular layer (MPa), h is the combined thickness of base and subbase layer, and $M_{R(support)}$ is the resilient modulus of subgrade as supporting layer. This is one of the major simplifications made in the Indian standard design code that takes into account equal material modulus of both the base and subbase layer. These materials shall be tested separately and pavement analysis and design shall be based on their evaluated resilient modulus. Material characterization of the unbound granular layer was solely based on CBR values of subgrade soil as resilient modulus tests using repeated tri-axial equipment are usually expensive. CBR tests on unsoaked local granular soil were performed. Table 4 presents the resilient modulus and Poisson's ratio values used for unbound granular layers in pavement analysis.

Since resilient modulus takes into account only the elastic deformation of the specimen and often underestimates material stiffness at higher temperatures. Therefore, the process of material stiffness modulus evaluation as suggested by flexible pavement design codes in India [29] is on the conservative side. Also, in the absence of triaxial testing equipment, the code suggests empirical equations that further question the reliability of evaluated material properties. Extensive studies beyond the elastic response of these materials at different test temperatures need to be performed for a better analysis of the stiffness modulus.

4. FE modelling of bituminous concrete pavement

FE modelling of bituminous concrete pavement is not a new technique for pavement response prediction. Many researchers [1,45–55] have developed similar models in the past and reported pavement response subjected to various loads, contact pressures, and material characteristics. Most of these models have been developed in European countries suited to load class, contact pressure, and material properties of their origin. Limited studies [1,50] are available in developing countries like India, Bangladesh, and Sri Lanka where mixed traffic offers a wide range of load classes and contact pressure. Also, material properties used in various layers change significantly with changes in source and need characterization and modelling for pavement response prediction.

A three-dimensional FE model of bituminous concrete pavement has been developed in this study using ABAQUS. The conventional geometric design consists of four different layers namely, bituminous concrete (including dense bituminous macadam), base layer, granular subbase layer, and compacted soil subgrade layer. The present study takes into consideration the elastic properties of granular unbound aggregate layers and subgrade layers while it considers linear viscoelastic properties of bituminous concrete layer based on creep compliance test data. The accuracy of the model depends on several parameters including material properties, number of elements considered in the FE model, degrees of freedom, contact stress distribution, and boundary conditions [51]. With the increase in number of structural elements being considered in the FE model and degrees of freedom, computational complexities increases. Various element types are used in the FE model to approximate model geometry and adjacent elements are connected with each other at the nodes. A node is a connecting point of elements in the FE model where degrees of freedom are defined. In India, FE modelling of bituminous concrete pavement is relatively a new topic

Table 4
Material properties of unbound granular layers.

S No.	Pavement layers	Thickness (mm)	Resilient modulus (MPa)	Poisson's ratio
1	Subgrade	500	87.25	0.35
2	Granular sub base	350	321.81	0.35
3	Granular base	300	321.81	0.35

of research and gaining interest with the success of consecutive modelling efforts. For the prediction of the structural response of bituminous concrete pavement using FE analysis, one needs to develop a pavement model, tire model, and material models for various layers. In developing nations like India, researchers have gained success in pavement modelling, however, material characterization and 3-dimensional modelling of test tire is relatively unexplored and has a lot to be done.

4.1. Pavement structure

In this study, stress has been given to LVE material characterization of bituminous mix for sensitivity analysis of the pavement response. In India, pavement design is based on linear elastic theory as selected in the guidelines for the design of flexible pavement (IRC: 37–2018).

The pavement structure consists of a 150 mm BC layer (including dense bituminous macadam), 300 mm aggregate base layer, 350 mm granular subbase layer, and 500 mm compacted subgrade layer.

The top surface of 150 mm BC was used to model the contact area for tire loading. The 20 kN tire load was assumed to be uniformly distributed over the contact area at the tire pavement interface. The contact area was estimated using a standard contact pressure of 560 kPa [29]. The contact area can be represented using a rectangle and two semi-circles at the ends as shown in Fig. 3(a). Further, this shape of the loading area is converted to an equivalent rectangle as suggested by Huang [56] having an area of 0.5227 L^2 and a width of 0.6 L. Dimensions of the contact area can be evaluated using tire load and contact pressure. The contact area was loaded using 560 kPa of contact pressure uniformly distributed over the entire area for validation of the FE model.

4.2. Loading and boundary conditions

Sufficient depth below the subgrade layer (7000 mm) has been provided to subside the pavement structural distresses to zero. Longitudinal and lateral movement of pavement elements has been restricted as it is infinite in length compared to small sections considered for analysis and laterally supported by shoulder or earthen soil. Ideally, movement of nodes in longitudinal (X) direction shall be allowed as it is free to move with vehicular loading. The structural response of the pavement was also evaluated with nodes having additional degrees of freedom in the X direction. It was found that, vertical deformation increases by 2.83% and compressive strain by 2.33%. Since this is not a significant change so movement of nodes in X direction was constrained to reduce computational efforts. Only vertical movement of integration points and elements is allowed as shown in Fig. 3(b). All nodes at the bottom plane have been restricted from the translational or rotational degrees of freedom.

The bituminous concrete pavement model was meshed after the evaluation of contact area dimensions and applying boundary conditions. The hexahedral elements type was used to mesh all the layers in the pavement. A finer mesh close to the loading area and a relatively coarser mesh size were used for the region away from the loading area.

5. Results and discussion

5.1. Creep compliance

A creep compliance test was conducted for the determination of the time-dependent response of BC-2 at three different air voids of 4%, 5%, and 6%. Samples have been tested at three different test temperatures of 5°, 15°, and 25° C against each air void. Horizontal and vertical deformations of the sample with temperature have been noted (see Fig. 4). It can be noted that as loading time increases, both horizontal and vertical deformation also increases. The gradient of the deformation-time graph is steeper at the beginning and gets flatter at the end. These deformations were also found to increase with air void and temperature. With the increase in temperature, the stiffness of the material decreases thus deformation is found to increase. Further, with the increase in air void in the mix, the density of the mix decreases which allows constituent particles to settle more easily into these voids, and deformations in the axial as well as lateral direction increases. Percentage change in deformation at each time step has been evaluated and shown for the temperature of 25° C compared to 15° C in Fig. 4.

The average annual temperature in India hovers around 25° C, so analysis is more focused on this temperature. Also, to maintain clarity in the figures, the percentage change in deformation at 15° C compared to 5° C has not been shown here. It can be seen from Fig. 4 that, the percentage change in deformation is continuously increasing with time. It shows, higher material stiffness at lower temperatures, and consecutively, the deformation plot flattens more quickly than at higher temperatures. A similar trend was not observed for 15° C temperature compared to 5° C. Percentage changes in deformation were relatively stable and constant. This may be due to at lower temperatures, change in material stiffness is relatively constant, and elastic deformation is more dominant than plastic deformation. These deformation data were used to find creep compliance of the material as per AASHTO T:322–07 [57]. Variation of creep compliance as a function of time at an air void of 4,5, and 6% and a temperature of 5°, 15°, and 25° C is shown in Fig. 5.

It can be seen from Figs. 4 and 5 that trends of creep compliance and deformation plots are simillar as they hold a proportionality relationship among them. Creep compliance data as fitted in the Prony series model shows good agreement with lab-calculated data at lower temperatures and variation increases at higher temperatures. It can be noted that a model that fits compliance data with great accuracy at lower temperatures may not fit well at higher temperatures. In this study, the Prony series model was fitted to consider the elastic stiffness of the material

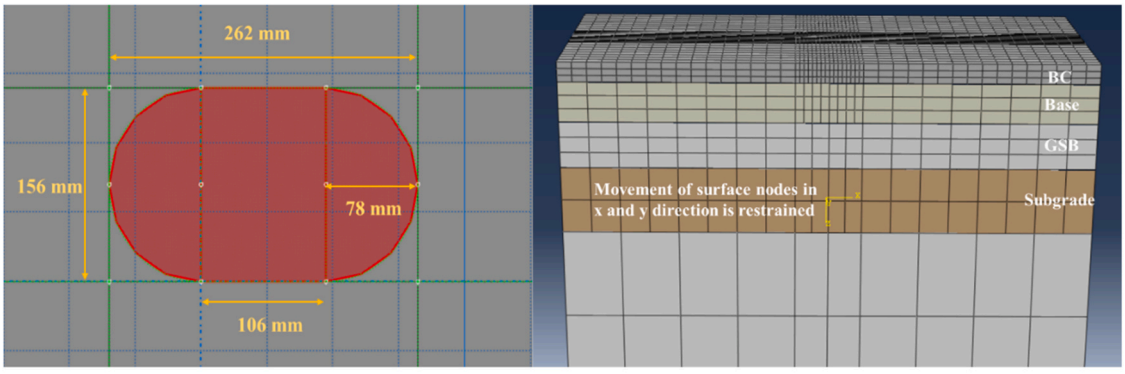

Fig. 3. (a) Contact area dimension (mm) for tire loading (b) Meshing in various layers and boundary conditions.

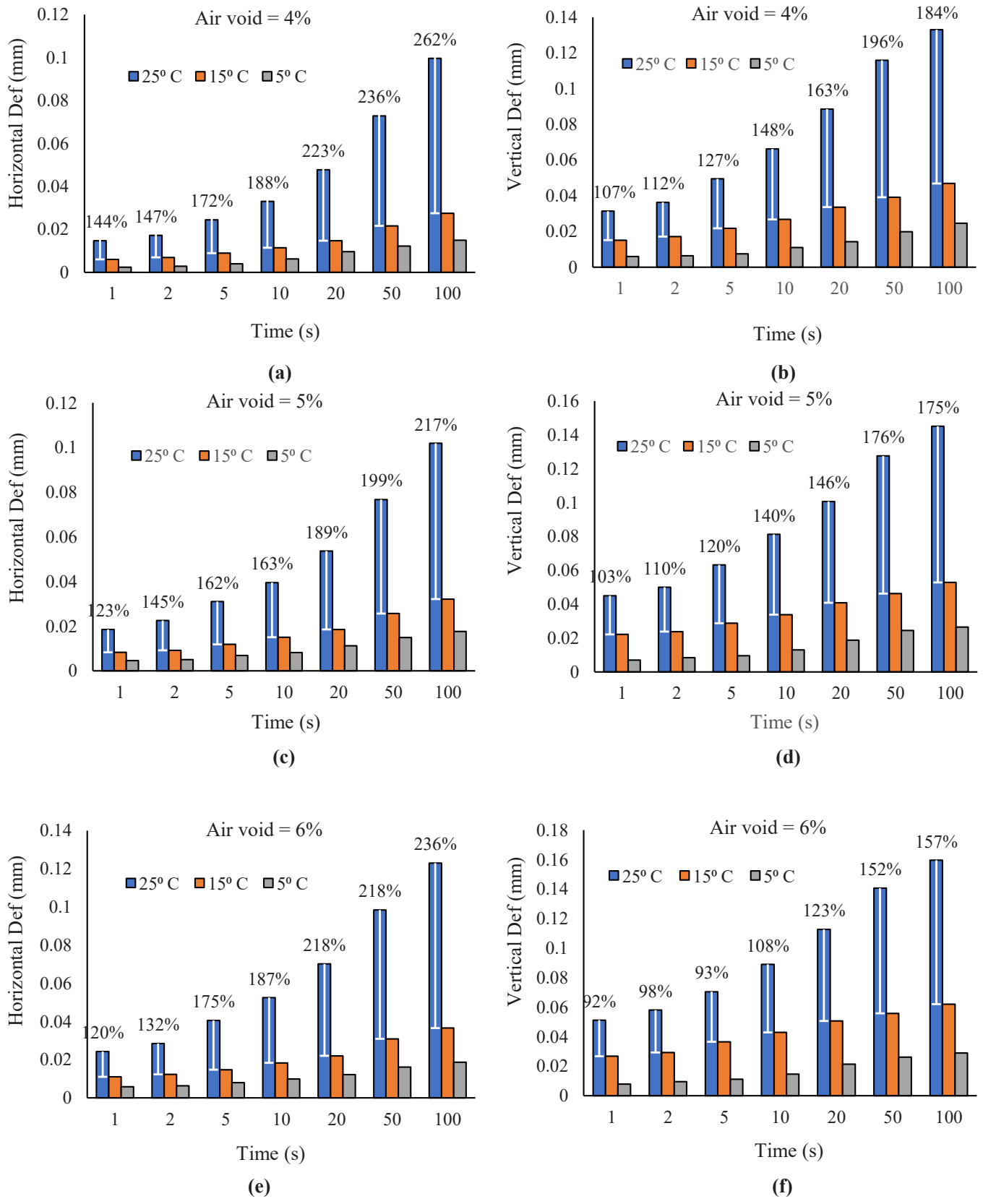

Fig. 4. Variation of horizontal and vertical deformations with time at different temperatures and air voids.

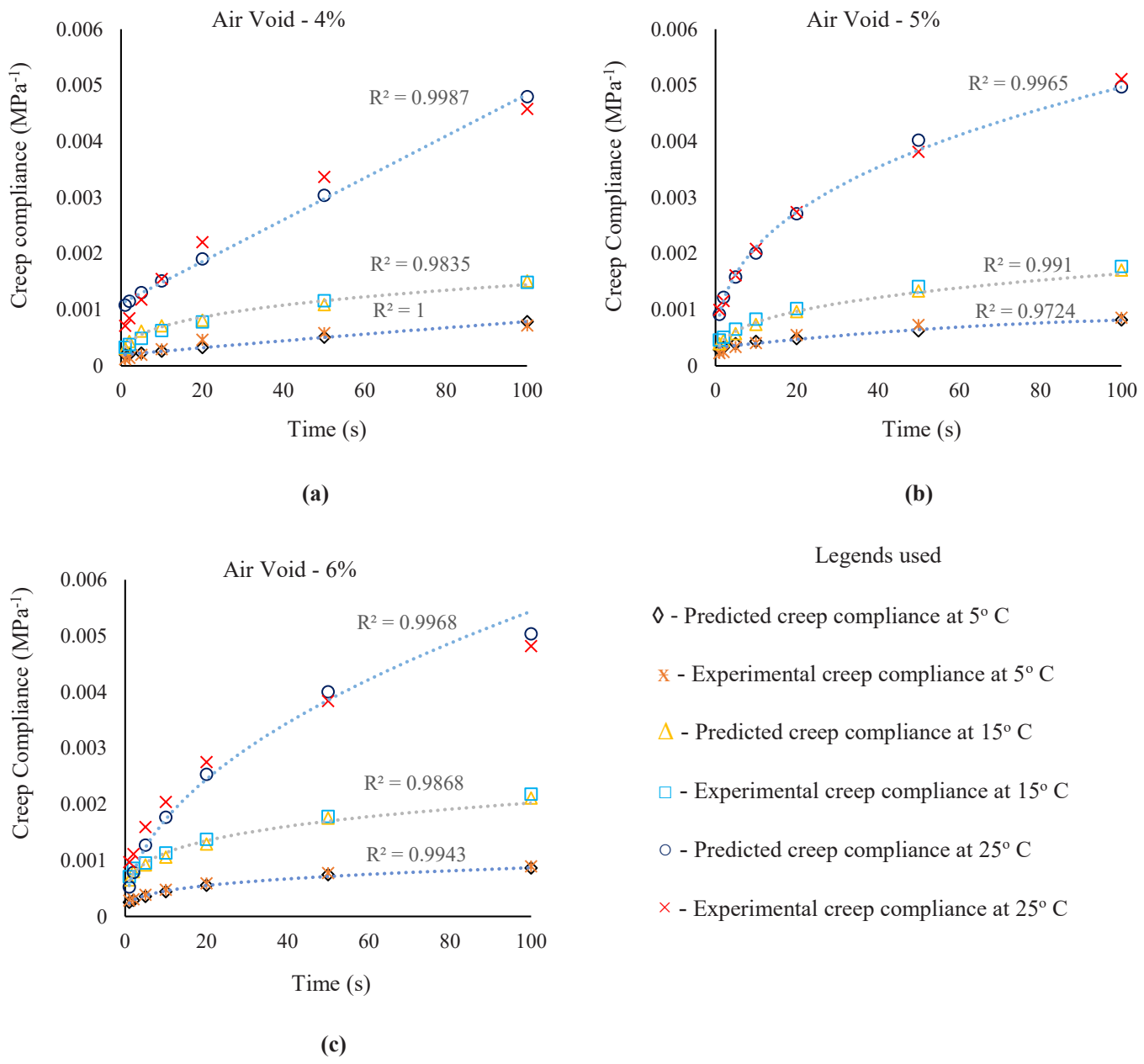

Fig. 5. Variation of creep compliance (experimental and model fit) with time at (a) 4% air void (b) 5% air void (c) 6% air void.

and hence it is not that accurate to consider plastic flow behaviour at a higher temperature.

Creep test results were also used to study the material stiffness using relaxation modulus. This relaxation modulus was used to further study the shear and bulk modulus of BC-2 material. Power law and the Prony series model were used to fit the relaxation modulus variation with time. Then, the time-dependent variation of shear modulus G(t) and bulk modulus K(t) were estimated assuming constant Poisson's ratio given by the following relation:

$$G(t) = \frac{E(t)}{2(1+\upsilon)} \tag{11}$$

$$K(t) = \frac{E(t)}{3(1-2\upsilon)} \tag{12}$$

Creep compliance fitted by Power law and Prony series is presented in Fig. 6(a) and (b) respectively. Relaxation modulus, shear modulus, and bulk modulus as predicted from Eqs. (7), (11), and (12) were plotted against reduced time and shown in Fig. 6(c) and (d).

The Power law model as shown in Fig. 6(a), is not a good fit of creep compliance data, as for a long period, there is almost no change in creep compliance and thereafter starts increasing with a steep gradient. It can be used to pre-smoothen the creep compliance data before fitting it to a Prony series model. Trends of creep compliance data as fitted in the Prony series model were found simillar as evaluated in the lab. So, the Prony series model was found to be a good fit for creep compliance data and can predict it well as a function of time as shown in Fig. 6(b). Further, relaxation, shear, and bulk modulus data were also fitted. Relaxation modulus was found to follow the inverse trend of relaxation modulus as shown in Fig. 6(c). Since shear and bulk modulus hold a proportional relation with relaxation modulus, their plot also follows a simillar trend as that of relaxation modulus as shown in Fig. 6(d). Plots of relaxation modulus, shear modulus, and bulk modulus can be classified into three zones. Zone 1 and 3 are identical in nature and reflect very small variations in modulus values with reduced time. Plots are relatively flatter in these zones. In zone 1, the material offers the highest

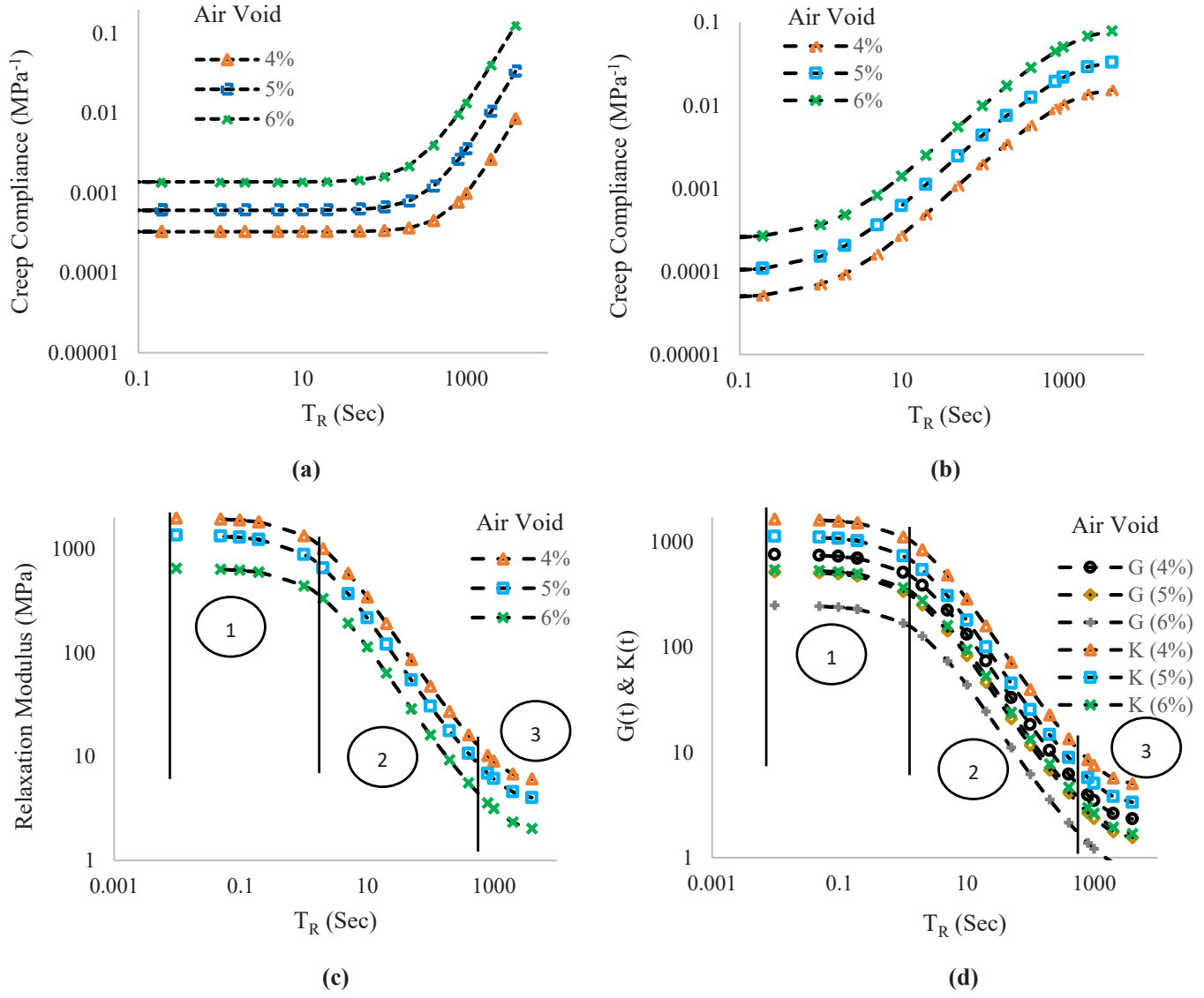

Fig. 6. Variation of creep compliance with time fitting (a) Power law (b) Prony series (c) Variation of relaxation modulus with time fitting Prony series (d) Variation of shear modulus and bulk modulus with time fitting Prony series.

resistance to the applied load and modulus values mobilise to maximum as constituent particles are intact in the mix. As time passes, particles start slipping from their original position and the modulus keeps on reducing in zone 2. At the end of zone 2, when the resilience of the material is negligible against applied load, a relatively flat plot is obtained in zone 3.

5.2. *Bituminous concrete pavement response*

After the evaluation of Prony series coefficients and the resilient modulus of unbound granular layers, the bituminous concrete pavement was modelled for structural response analysis. Pavement response as obtained from FE-based tool ABAQUS was first validated using 3D Move Analysis, a continuum-based finite layer approach software developed by the University of Nevada, Reno. FE model was validated considering the elastic properties of the bituminous mix. A validated model was used to predict pavement response in terms of normal compressive stress (σ_z), normal compressive strain (ε_z), and vertical deformation. These responses have been estimated at zero radial distance from the axle load (r = 0), and in a vertically downward direction along the pavement depth (z – z). Compressive stress has been considered positive while tensile stress as negative. A similar sign convention for strain has been followed. The sign convention used in the study is shown below.

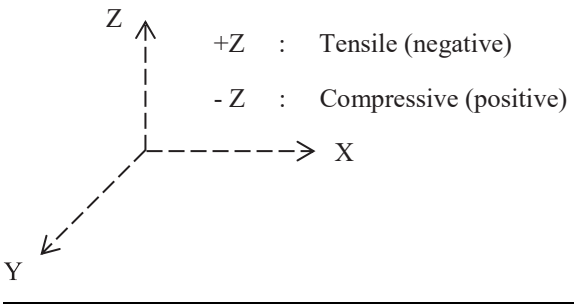

Different load classes of 20, 25, and 30 kN have been considered for pavement response sensitivity analysis. This load class corresponds to a single wheel load. Considering dual wheel assembly, the load shared by a single wheel is 20 kN, and the equivalent standard axle load considered for pavement design in India is 80 kN [29]. Considering the heavy truck tire loads that are frequent in India, wheel loads of 25 kN and 30 kN have also been considered for analysis. State highways and

national highways cater mixed traffic in India and allow movement of all categories of vehicles on the same lane where multiple lanes are not provided. Mixed traffic offers a wide range of wheel bases for different vehicles and thus contact pressure also changes. For pavement design in India, the standard contact pressure of 560 kPa is used. Contact stress distribution was analysed for 20 kN tire load. It was observed that the maximum contact pressure developed in the mid-section of the tire-pavement contact patch was 740 kPa and had an average value of 420 kPa. Therefore, three different contact pressures of 420, 560, and 740 kPa were selected for pavement analysis.

5.2.1. Effect of air void in the BC mix

The model uses the linear viscoelastic properties of bituminous concrete mix and resilient modulus properties of unbound granular layers. Pavement response was analysed to evaluate the effect of LVE properties of bituminous concrete and sensitivity with changes in air void, vertical load, contact pressure, and temperature. The plot of vertical deformation and normal compressive stress, σ_z (z-z) against pavement depth at 4%, 5%, and 6% air void has been presented in Fig. 7. σ_z has been plotted at log scale as the stress gradient is steep and reduces significantly in a small vertical depth domain.

The rate at which σ_z subsides initially against pavement depth is steeper than deformation. The stress reduction of 65.74%, 58.68%, and 55.53% was observed at air voids of 4%, 5%, and 6% respectively in the BC-2 layer. This is because the top layer of BC-2 has the highest stiffness among all the layers and is much higher than its subsequent base layer. So, most of the stress is taken by the bituminous concrete layer. It was also interesting to note that at a higher air void in the mix, the percent reduction in stress in the BC-2 layer was lesser than at a lower air void. This is due to the higher stiffness of the mix at lower air void giving a more compact structure and thus stress dissipates more quickly within the layer. Whereas, the opposite trend prevails in the case of deformation. As the material stiffness of the upper layers is higher than lower layers, so, the rate of subsidence of deformation is much lesser in BC-2 and base layers. Only 33.83%, 28.10%, and 23.27% of stress were reduced corresponding to 4%, 5%, and 6% of air voids in these layers, and most of the surface deformation was found to subside in the natural subgrade and compacted subgrade layers.

5.2.2. Effect of loading

The sensitivity of pavement response was further analyzed at different vertical loads and contact pressure. Load sensitivity analysis was performed corresponding to a vertical load of 20, 25, and 30 kN keeping other parameters of the FE model constant. Pavement response in terms of normal compressive stress (z-z), normal compressive strain (z-z), and vertical deformation for the full depth pavement, and BC-2 layer is shown in Fig. 8 for a contact pressure of 740 kPa.

It is important to note that, σ_z at a lower load (20 kN) is higher than σ_z at higher loads (25 and 30 kN) near the surface of the BC layer. After that, σ_z starts decreasing with the depth of the pavement and the reverse is true, i.e.,. σ_z at higher load (30 kN) is higher than stress at lower loads (20 and 25 kN). Response in other lower layers like granular base, subbase, and subgrade layers was found unidirectional. Normal compressive stress and normal compressive strain decreases throughout the depth of the layer however at the interface, normal compressive strains were found to increase sharply due to change in material properties. It can be concluded from Fig. 8 that, variations in stress and strains in lower granular layers at different load classes are more distinct than in upper bituminous concrete layer as the stiffness of granular layers is lesser. Although stresses coming to lower layers also reduces with depth, however, these are more susceptible to visible changes with different load classes.

5.2.3. Effect of contact pressure

FE model of bituminous concrete pavement was used for pressure sensitivity analysis at three different contact pressures of 740, 560, and 420 kPa at a constant vertical load of 20 kN as shown in Fig. 9. Here, variation has been shown for full depth pavement and bituminous concrete layer only. For pressure sensitivity analysis, it is interesting to note that, unlike load sensitive response, variation of σ_z and ε_z in the bituminous concrete layer is more distinct and shows more vertical gap between consecutive curves. However, the reverse is the case with lower granular layers. Response at different contact pressures in granular layers seems much closer and overlapping. It can be concluded that the BC-2 layer is more sensitive to contact pressure than vertical load.

In previous sections, the effect of tire load, contact pressure, and air void on the structural response of the pavement layers has been discussed. A comparative analysis of these responses among various layers has been presented in Table 5 and Table 6. The effect of contact pressure and axle load on pavement response has been presented quantitatively in Table 5. Maximum normal compressive stress (σ_z), normal compressive strain (micro-strain, ε_z), and vertical displacement were found in each layer of the pavement and presented in tabular forms. These responses were noted at the top of the surface course (z = 0), and interfaces of the pavement layers (z = 150, 450, and 800 mm).

It was found that σ_z and micro-strains (ε_z) are maximum in the BC layer followed by a sharp decrease in lower unbound granular layers. This is because the load is directly coming over the BC layer so it is

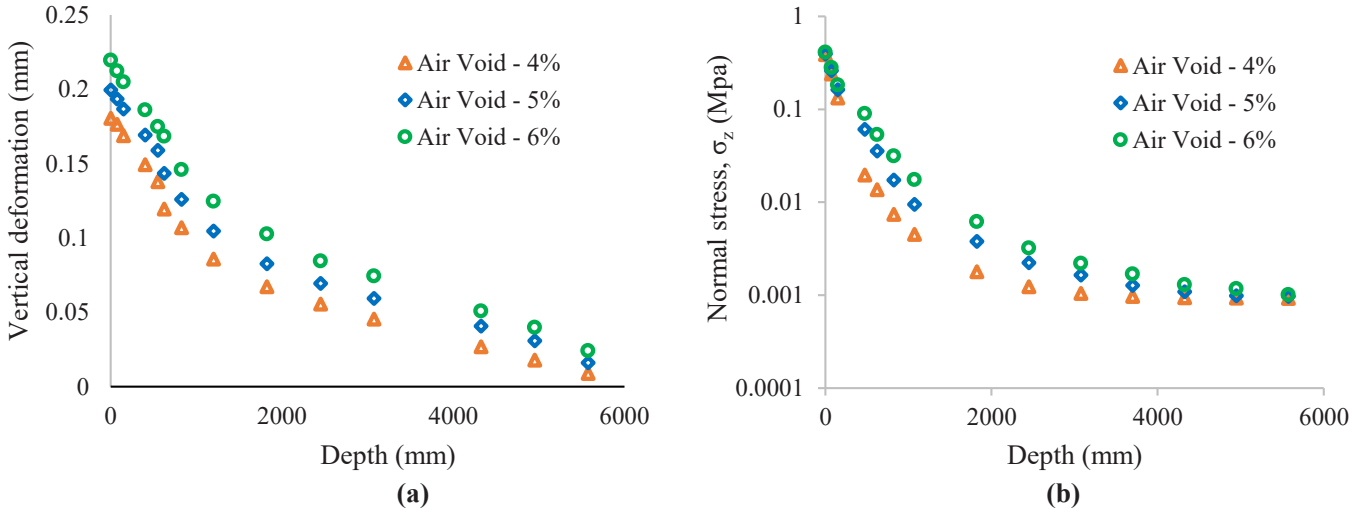

Fig. 7. (a) Pavement deformation vs. vertical depth (b) Normal compressive stress vs. pavement depth.

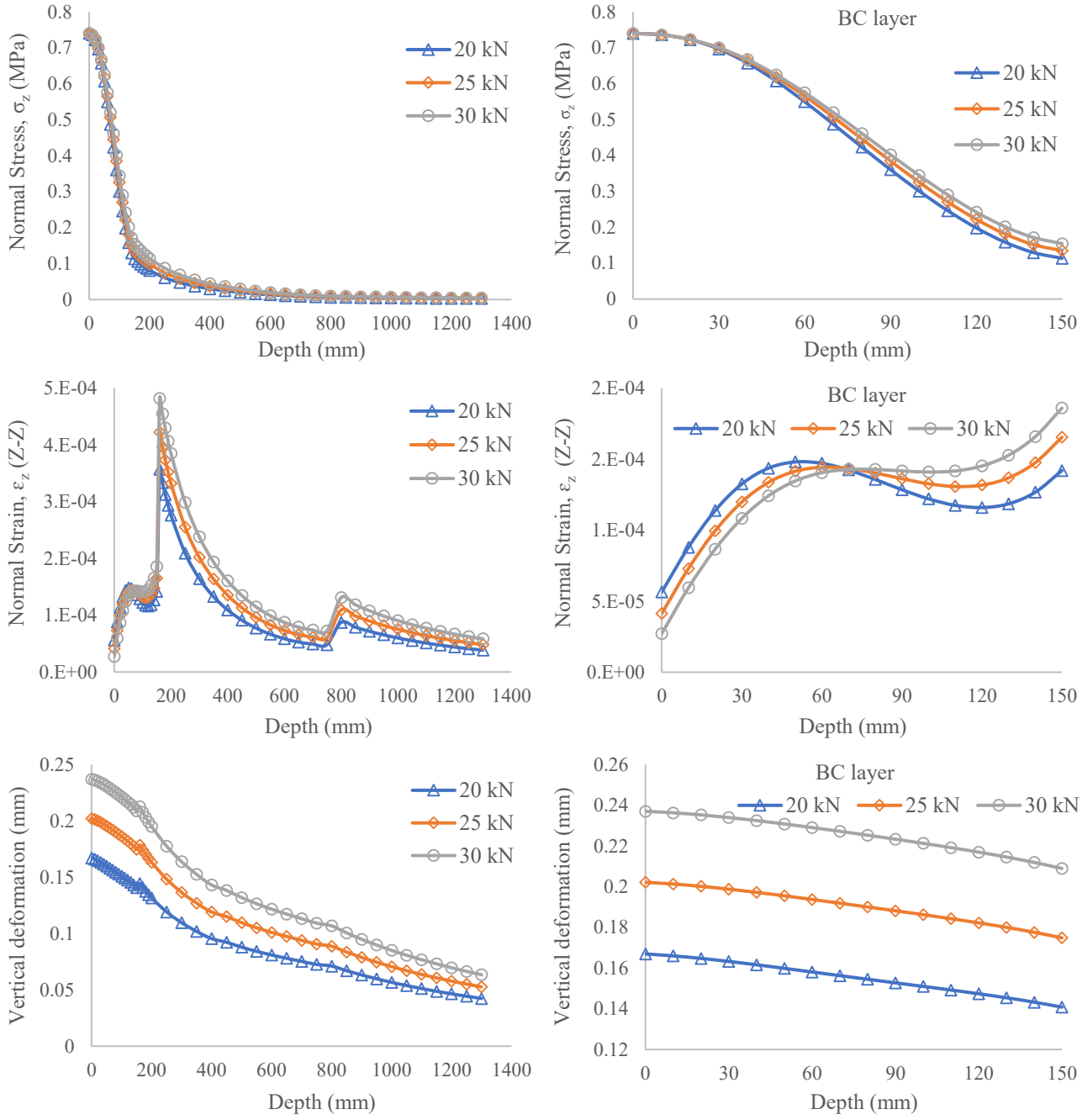

Fig. 8. Pavement response as normal compressive stress, normal compressive strain, and vertical deformation for full depth pavement and BC layer at a vertical load of 20, 25, and 30 kN.

subjected to maximum stress value. Also, the stiffness of the BC layer is much higher than lower granular layers so most of the stresses are absorbed by the BC layer only. Also, micro-strains calculated through out the pavement depth were found to decrease, however, a sharp increase was observed at the layer interface. Since the resilient modulus of various materials in the pavement layers kept on decreasing so normal compressive strain values at interfaces were significantly higher. It was also noted that the effect of varying load and the contact pressure is least significant for lower layers of GSB and subgrade layers as most of the stress is being taken by upper layers having higher modulus values.

The effect of air voids in BC mix and test temperature was also studied and presented in Table 6. Creep compliance test for BC mix was conducted at 5, 15, and 25° C only however looking into the temperature variation over the year in India, creep compliance data with time was also evaluated for a temperature of 40° C using Williams-Landel-Ferry (WLF) equation [58]. The WLF equation allows for the estimation of material properties beyond test data.

It can be seen from Table 6 that the effect of air void on the structural response of the BC mix is significant. Stresses in the BC layer are 11.58% higher when compacted with 5% air void as compared to 4%. This increase in stress rises to 23.06% when compacted with 6% air void. Vertical displacement in the BC layer observed was also significant. A rise of 21.14% was found in the displacement of the BC layer when the air void in the mix increased from 4% to 6%. The effect of temperature on the vertical displacement of pavement layers especially the BC layer was found significant. An increase in displacement of nearly 52.27% was found in the BC layer when the temperature rises from 5° C to 40° C.

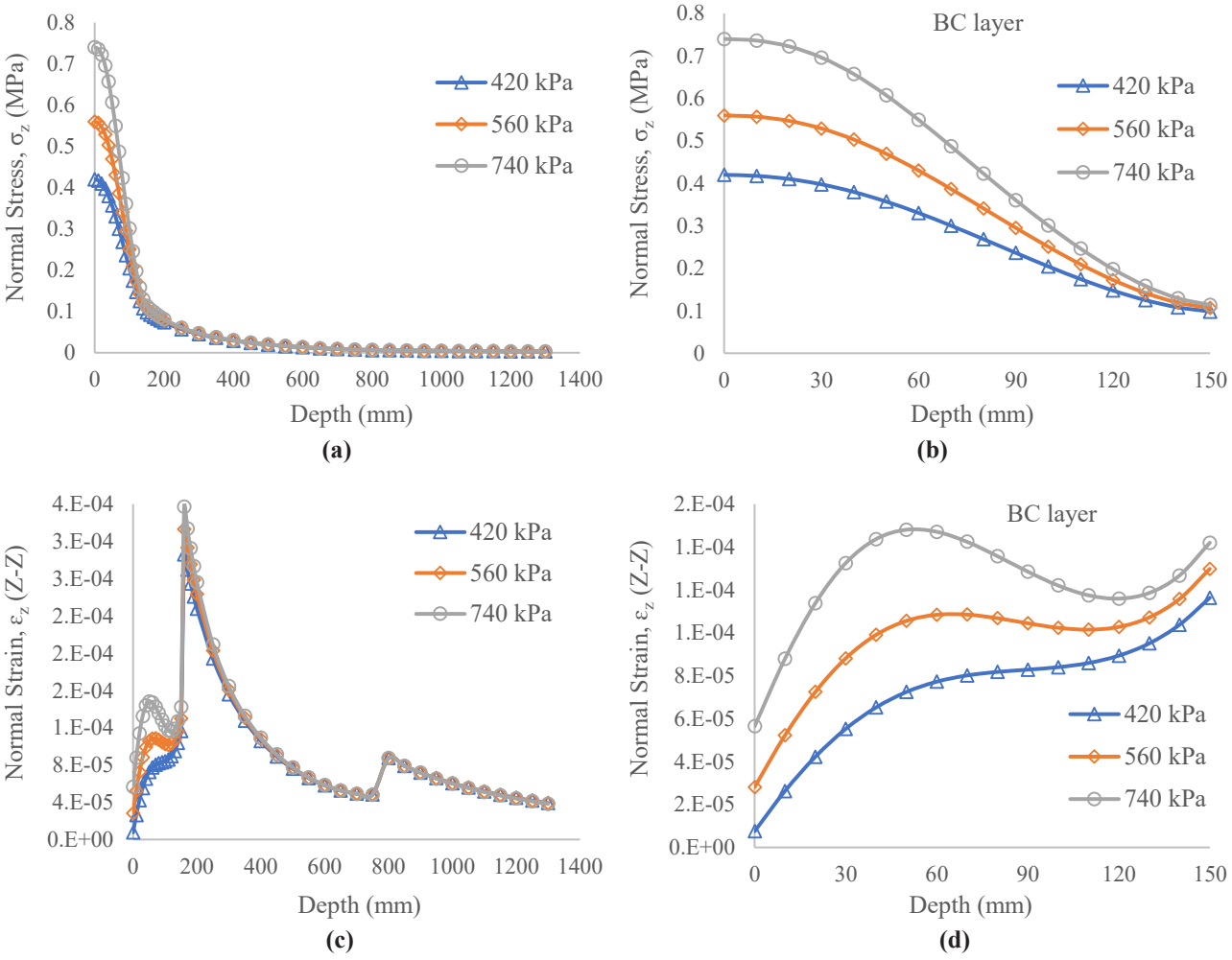

Fig. 9. Pavement response as normal compressive stress and normal compressive strain in z-z direction for full depth pavement and bituminous concrete layer at a contact pressure of 420, 560, and 760 kPa.

5.2.4. Effect of loading on critical mechanistic parameters

The vertical compressive strain on top of the subgrade and horizontal tensile strain at the bottom of the bituminous layer are considered to be critical mechanistic parameters for controlling subgrade rutting and bottom-up cracking in the bituminous layer respectively. The effect of loading on these parameters was identified as shown in Table 7.

Tensile strain (ε_t) at the bottom of the BC layer was found to increase by 37.76% when the vertical load on the pavement rises from 20 kN to 30 kN. Tensile stress (σ_t) almost in the same proportion was found to increase by 35.97% with the same change in load magnitude. The other important mechanistic parameter, vertical compressive strain at the top of the subgrade, ε_z (z = 800 mm) was found to increase by 54.63% when the load changes from 20 kN to 30 kN. So, the effect of load on ε_z was more prominent than ε_t. These critical mechanistic parameters were used to find the rutting and fatigue performance of the BC pavement. Rutting and fatigue performance models (Eq. 13 & 14) as provided in IRC:37 guidelines with 90% reliability were used to estimate the subgrade rutting life and fatigue life of the BC layer for a standard axle load of 80 kN.

$$N_r = 1.4100 \times 10^{-8} \left(\frac{1}{\varepsilon_z}\right)^{4.5337} \tag{13}$$

Where N_r is subgrade rutting life (cummulative equivalent number of 80 kN standard axle loads that can be served by the pavement before the critical rut depth of 20 mm or more occurs), and ε_z is the vertical compressive strain at the top of the subgrade layer.

$$N_f = 0.5161 \times C \times 10^{-4} \left(\frac{1}{\varepsilon_t}\right)^{3.89} \times \left(\frac{1}{M_{RM}}\right)^{0.854} \tag{14}$$

$$Where \quad C = 10^{M}, and \quad M = 4.84\left(\frac{V_{be}}{V_a + V_{be}} - 0.69\right)$$

Where V_a is % volume of air void in the BC mix, V_{be} is % volume of effective bitumen in the mix, N_f is the fatigue life of the BC layer, ε_t is the maximum horizontal tensile strain at the bottom of the BC layer, C is an adjustment factor used to account for the effect of variation in the mix volumetric parameters, and M_{RM} is the resilient modulus of BC mix.

These empirical relations were used to find the rutting and fatigue performance of the BC pavement corresponding to a standard axle load of 80 kN only as these relations are designed for standard axle load only. The BC pavement was found to perform excellent against both of these failure criteria. Subgrade rutting life was found to be 3986 msa whereas fatigue life of the BC layer was found to be 73 msa.

5.3. Statistical analysis

Two-way Analysis of Variance (ANOVA) was carried out to study the effect of load and contact pressure on the stresses (σ_z) and strains (ε_z) at different pavement depths. Load and contact pressure were considered as the independent variables whereas stresses and strains at different

Table 5
Effect of contact pressure and load on the structural response of various layers of BC pavement.

Contact pressure (kPa)	Pavement layer	σ_z (kPa)	% decrease	Micro-strain	% decrease
420	BC	420.0		116.36	
	Base	98.21	76.61	305.93	-61.96
	GSB	23.97	94.29	89.05	23.47
	Subgrade	6.56	98.43	87.26	25.0
560	BC	560.0		129.83	
	Base	106.36	81.0	333.12	-61.02
	GSB	24.33	95.65	90.36	30.40
	Subgrade	6.59	98.82	87.39	32.68
740	BC	740.0		148.07	
	Base	113.57	84.65	357.03	-58.53
	GSB	24.60	96.67	91.25	38.37
	Subgrade	6.61	99.10	87.30	41.04
Load (kN)	Pavement layer	σ_z (kPa)	% decrease	Micro-strain	% decrease
20	BC	740.0		148.07	
	Base	113.57	84.65	357.03	-58.52
	GSB	24.60	96.67	91.25	38.37
	Subgrade	6.61	99.10	87.30	41.04
25	BC	740.0		165.42	
	Base	134.82	81.78	422.63	-60.86
	GSB	30.49	95.88	113.21	31.56
	Subgrade	8.24	98.88	109.24	33.96
30	BC	740.0		185.97	
	Base	154.27	79.15	482.13	-61.43
	GSB	36.28	95.09	134.76	27.54
	Subgrade	9.86	98.66	131.05	29.53

Table 6
Effect of air void and temperature on the structural response of various layers of BC pavement.

Air void (%)	Pavement layer	σ_z (kPa)	% decrease	Vertical displacement (mm)	% decrease
4	BC	740.0		0.175	
	Base	113.57	84.65	0.149	14.85
	GSB	24.60	96.67	0.121	30.85
	Subgrade	6.61	99.10	0.089	49.14
5	BC	740.0		0.193	
	Base	126.18	82.94	0.169	12.43
	GSB	28.35	96.17	0.142	26.42
	Subgrade	7.92	98.93	0.104	46.11
6	BC	740.0		0.212	
	Base	146.18	80.24	0.186	12.26
	GSB	33.02	95.53	0.163	23.11
	Subgrade	9.12	98.77	0.112	47.17
Temperature (°C)	Pavement layer	σ_z (kPa)	% decrease	Vertical displacement (mm)	% decrease
5	BC	740.0		0.176	
	Base	91.17	87.68	0.151	14.20
	GSB	17.22	97.67	0.120	31.81
	Subgrade	5.38	99.27	0.085	51.70
15	BC	740.0		0.198	
	Base	99.28	86.58	0.152	23.23
	GSB	20.12	97.28	0.123	37.88
	Subgrade	5.94	99.19	0.088	55.55
25	BC	740.0		0.232	
	Base	113.57	84.65	0.154	33.62
	GSB	24.60	96.67	0.126	45.69
	Subgrade	6.61	99.10	0.092	60.34
40	BC	740.0		0.268	
	Base	138.4	81.29	0.156	41.79
	GSB	29.78	95.97	0.128	52.24
	Subgrade	7.98	98.92	0.094	64.92

depths were taken as dependent variables. Table 8 presents the results of the statistical analysis at a 95% confidence level ($\alpha = 0.05$). It is noted that the effect of independent variables is significant when the p-value is less than 0.05. Both independent variables i.e., loads and contact pressure have a significant impact on dependent variables (see Table 8). This shows the importance of these parameters in governing the design of bituminous concrete pavement.

Table 7
Effect of loading on critical mechanistic parameters considered for pavement design.

Load (kN)	Depth, Z (mm)	Tensile stress, σ_t (kPa)	Compressive strain, ε_z (micro-strain)	Tensile strain, ε_t (micro-strain)
20	150	543.5	390.0	150.4
	800	21.79	141.5	67.86
25	150	647.3	471.0	180.4
	800	24.33	180.3	73.50
30	150	739.0	545.7	207.2
	800	30.20	218.8	89.15

Table 8
Summary of Two-way ANOVA at 95% confidence level.

Variables	Source of variation	F calculated	P-value	F critical
σ_z at 100 mm	Contact pressure	12543.81	3E-08	6.94
	Load	0.71	0.542	6.94
σ_z at 150 mm	Contact pressure	158.88	0.00015	6.94
	Load	19.44	0.01	6.94
σ_z at 300 mm	Contact pressure	51.49	0.0014	6.94
	Load	57.68	0.0011	6.94
σ_z at 800 mm	Contact pressure	26.21	0.0050	6.94
	Load	1611.58	0.000002	6.94
ε_z at 100 mm	Contact pressure	9130.2	5E-08	6.94
	Load	278.3	5E-05	6.94
ε_z at 150 mm	Contact pressure	294.03	0.0004	6.94
	Load	220.1	0.039	6.94
ε_z at 300 mm	Contact pressure	52.6	0.0013	6.94
	Load	51.1	0.0014	6.94
ε_z at 800 mm	Contact pressure	14.21	0.015229	6.94
	Load	973.17	0.000004	6.94

It can be seen that contact pressure has a significant effect on σ_z and ε_z at each point whereas load has a significant effect on these parameters except at 100 mm depth (as p-value > 0.05). This is mainly due to the presence of a viscoelastic bituminous layer up to 150 mm depth in which tensile strain starts building nearly 50 mm. Additionally, this might be due to the load levels within the linear viscoelastic regime for the bituminous layer.

To better understand the significance of these variables on stresses and strains, main effect plots were plotted at a 95% confidence level. The results for other depths are not shown here for brevity. Fig. 10 shows the change in dependent variables with the variation in the attributes of independent variables.

6. Conclusions

The correct characterization of mechanical properties of BC mixes is important for predicting the accurate lifetime expectancy of the flexible pavements particularly, under Indian design specifications. Current standard specifications are primarily based on characterizing the BC material as elastic. In order to obtain these mechanical behaviours, resilient modulus tests are recommended. Several studies reported that characterizing BC material with only elastic properties induces uncertainty in the prediction of an expected lifetime. Although modern-day computational tools allow input of complex material characterization such as viscoelastic/visco-elasto-plastic etc. but they generally require specific input parameters. To the best of the authors' knowledge, there are very few studies that tried to develop a framework to obtain visco-elastic characterization of BC mixes under Indian conditions. The present study proposed a framework to obtain and evaluate Prony series parameters for the BC mixes on the basis of creep compliance tests performed for different compositions of mixes (air voids: 4%, 5%, and

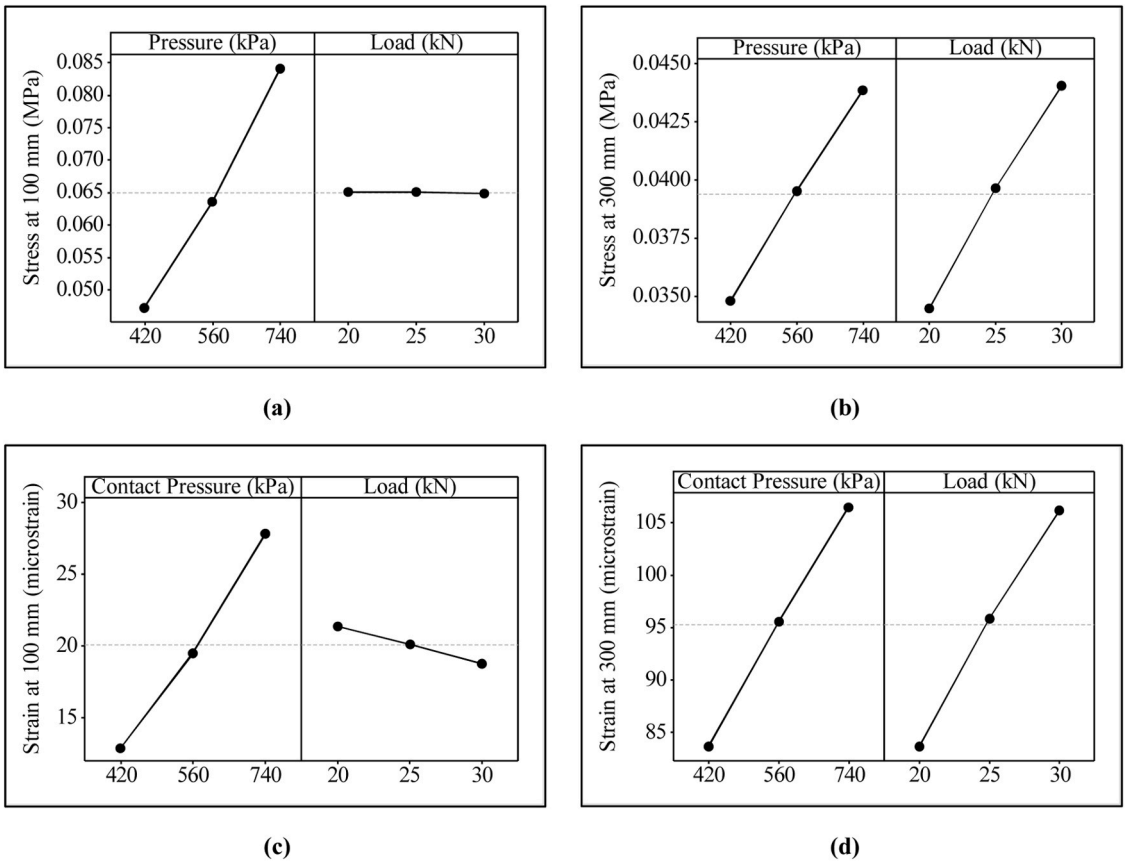

Fig. 10. Main effect plots for stress and strain at 100 mm and 300 mm depth.

6%) and temperatures (5, 15, and 25° C).

As a next step 3-dimensional FE models were developed to obtain sensitivity of critical stresses (σ_z) and strains (ε_z) in different layers with the variation of load types (20, 25, and 30 kN), contact pressures (420, 560, 740 kPa), air voids (4%, 5%, and 6%) and temperatures (5, 15, 25, and 40° C). Key conclusions are highlighted below:

- From load and pressure sensitivity analysis, it was found that the effect of contact pressure variation on the structural response of pavement layers is more prominent than load in the surface layer of the BC pavement. An increase in ε_z of 27.25% in the BC layer was found when contact pressure changed from 420 kPa to 740 kPa however an increase in ε_z was found to be 25.59% when load was changed from 20 kN to 30 kN. Though the effect of contact pressure seems higher but further analysis is required to make a comparative analysis. In the present study, % change in contact pressure is also higher than % change in load so it may cause a higher impact on the pavement response. This highlights the importance of considering vehicle tire type and stress distribution at tire-pavement contact during analysis.

- -Change in temperature was found to have a significant influence on vertical deformation in the BC layer. For example, vertical displacement was found to increase by 52.27% in the BC layer when temperature was changed from 5° C to 40° C. This highlights the importance of consideration of region (based on temperature) in the design process.
- -Change in air voids in the BC mix also plays a vital role in the pavement design stage itself as it affects the critical structural response of the BC layer considerably. It was found that an increase in air void from 4% to 6% increases vertical displacement by 21.14% and normal compressive stress by 23.06%. It shows the importance of BC mix compaction in the field. Good construction practices such as adequate compaction play a significant role in achieving the desired lifetime.
- -It was also noted that the variation in structural response was found to be in agreement with past literatures i.e., the least for lower layers of GSB and subgrade.

In the last step, Two-way ANOVA was carried out to see the relative effects of contact pressure and vertical loading on the structural response of the pavement. It was observed that pavement response is more sensitive to contact pressure than vertical loading. It may be due to variation in pressure selected as input parameter were higher than load. Further, the effect of load at the mid-section of the bituminous concrete section was not found significant however, the same is not true for contact pressure.

In general, this research is an attempt to present a FEM-based simple and practical framework to evaluate the structural response of BC material with viscoelastic material characterization which can be an effective tool to predict field behaviour with commonly available pavement material tests. Such a framework could be a very useful tool for practitioners and researchers.

Future scope of the study

To make the study more inclusive and comprehensive, other ranges of temperature and air void shall be included. It will make analysis more effective in the sense of understanding material properties with more clarity. Additionally, the tire footprint considered for loading uniformly distributes contact stresses which is not the actual condition in the field. In a further study, we shall simulate actual tire contact and contact stress distribution. Also, the resilient modulus approach used for unbound granular layers underestimates layer stiffness at higher temperatures.

Future studies should explore the material nonlinearity effect on pavement response.

CRediT authorship contribution statement

Kumar Abhinav: Writing – original draft, Visualization, Validation, Software, Methodology, Funding acquisition, Formal analysis, Data curation, Conceptualization. **Gupta Ankit:** Writing – review & editing, Visualization, Supervision, Resources, Methodology, Investigation, Conceptualization. **Anupam Kumar:** Writing – review & editing, Visualization, Supervision, Software, Methodology, Investigation, Formal analysis, Conceptualization. **Wagh Vivek Pratap:** Writing – review & editing, Visualization, Methodology, Data curation, Conceptualization.

Declaration of Competing Interest

The authors declare the following financial interests/personal relationships which may be considered as potential competing interests. Abhinav Kumar reports financial support was provided by MHRD, India. Abhinav Kumar reports a relationship with Indian Institute of Technology BHU Varanasi that includes: non-financial support.

Data availability

Data will be made available on request.

References

[1] M.S. Ranadive, A.B. Tapase, Parameter sensitive analysis of flexible pavement, Int. J. Pavement Res. Technol. vol. 9 (6) (. 2016) 466–472, https://doi.org/10.1016/j.ijprt.2016.12.001.

[2] Á. Holanda, E. P. Junior, and T. Araújo, Finite element modeling of flexible pavements, no. September, 2006, [Online]. Available: http://repositorio.ufc.br:8080/ri/handle/123456789/1380.

[3] A. Ghosh, A. Padmarekha, J.M. Krishnan, Implementation and proof-checking of mechanistic-empirical pavement design for indian highways using aashtoware pavement ME design software, Procedia Soc. Behav. Sci. vol. 104 (. 2013) 119–128, https://doi.org/10.1016/j.sbspro.2013.11.104.

[4] MoRTH, Specifications for road and bridge work (Fifth revision), New Delhi, 2013.

[5] M.J. Williamson, Finite element analysis of hot-mix asphalt layer interface bonding, 2015.

[6] Y.-R. Kim, D.N. Little, Linear viscoelastic analysis of asphalt mastics, J. Mater. Civ. Eng. vol. 16 (2) (. 2004) 122–132, https://doi.org/10.1061/(ASCE)0899-1561(2004)16:2(122).

[7] C.Y. Cheung, D. Cebon, Experimental study of pure bitumens in tension, compression, and shear, J. Rheol. (N. Y N. Y) vol. 41 (1) (. 1997) 45–74, https://doi.org/10.1122/1.550858.

[8] Y.T. Chou, H. Larew, Stresses and displacements in viscoelastic pavement systems under a moving load, Transp. Res Rec. (1969) 25–40.

[9] J.F. Elliott, F. Moavenzadeh, Analysis of stresses and displacements in three-layer viscoelastic systems, Highw. Res. Rec. (1971).

[10] Y.H. Huang, Stresses and strains in viscoelastic multilayer systems subjected to moving loads, Highw. Res. Rec. (457) (1973) 60–71.

[11] S.W. Park, Y.R. Kim, Analysis of layered viscoelastic system with transient temperatures, J. Eng. Mech. vol. 124 (2) (1998) 223–231, https://doi.org/10.1061/(asce)0733-9399(1998)124:2(223).

[12] R.A. Schapery, A method of viscoelastic stress analysis using elastic solutions, J. Frankl. Inst. vol. 279 (4) (1965) 268–289, https://doi.org/10.1016/0016-0032(65)90339-X.

[13] P. Mackiewicz, A. Szydło, Viscoelastic parameters of asphalt mixtures identified in static and dynamic tests, Materials vol. 12 (13) (2019), https://doi.org/10.3390/ma12132084.

[14] M.A. Elseifi, I.L. Al-Qadi, P.J. Yoo, Viscoelastic modeling and field validation of flexible pavements, J. Eng. Mech. vol. 132 (2) (2006) 172–178, https://doi.org/10.1061/(ASCE)0733-9399(2006)132:2(172).

[15] L. Zhang, X. Zhang, X. Liu, Y. Luo, Viscoelastic model of asphalt mixtures under repeated load, J. Mater. Civ. Eng. vol. 27 (10) (2015) 04015007, https://doi.org/10.1061/(asce)mt.1943-5533.0001256.

[16] M.W. Witczak, T.K. Pellinen, M.M. El-Basyouny, Pursuit of the simple performance test for asphalt mixture rutting. Asphalt Paving Technology 2002, Association of Asphalt Paving Technologists (AAPT), Colorado, 2002, pp. 767–778.

[17] M. Jeong, Comparison of Creep Compliance Master Curve Models for Hot Mix Asphalt, 2005.

[18] Shell International Petroleum Company, Shell pavement design manual: Asphalt pavements and overlays for road traffic, 1978.

[19] Thickness design-Asphalt pavements for highways and streets, 9th Ed, Lexington, KY, 1999.

[20] H.L. Theyse, M. De Beer, F.C. Rust, Overview of South African mechanistic pavement design method, Transp. Res. Rec.: J. Transp. Res. Board vol. 1539 (1) (1996) 6–17, https://doi.org/10.1177/0361198196153900102.

[21] A. Gupta, A. Kumar, Comparative structural analysis of flexible pavements using finite element method, Int. J. Pavement Eng. Asph. Technol. vol. 15 (1) (2015) 11–19, https://doi.org/10.2478/ijpeat-2013-0005.

[22] M.A. Elseifi, I.L. Al-Qadi, P.J. Yoo, Viscoelastic modeling and field validation of flexible pavements, J. Eng. Mech. vol. 132 (2) (2006) 172–178, https://doi.org/10.1061/(ASCE)0733-9399(2006)132:2(172).

[23] I.L. Al-Qadi, M. Elseifi, and P.J. Yoo, In-situ validation of mechanistic pavement finite element modeling, in International Conference on Accelerated Pavement Testing, Minneapolis, Minnesota, USA, 2004.

[24] S.W. Park, R.A. Schapery, Methods of interconversion between linear viscoelastic material functions. Part I—a numerical method based on Prony series, Int J. Solids Struct. vol. 36 (11) (1999) 1653–1675, https://doi.org/10.1016/S0020-7683(98)00055-9.

[25] L. Zhang, X. Zhang, C. Hu, Deformation Prediction of Asphalt Mixtures under Repeated Load Base on Viscoelastic Mechanical Model. Paving Materials and Pavement Analysis, American Society of Civil Engineers, Reston, VA, 2010, pp. 116–125, https://doi.org/10.1061/41104(377)15.

[26] D.N. Richardson and S.M. Lusher, Determination of Creep Compliance and Tensile Strength of Hot-Mix Asphalt for Wearing Courses in Missouri, Apr. 2008.

[27] M. Nasimifar, S. Thyagarajan, N. Sivaneswaran, Backcalculation of flexible pavement layer moduli from traffic speed deflectometer data, Transp. Res. Rec.: J. Transp. Res. Board vol. 2641 (1) (2017) 66–74, https://doi.org/10.3141/2641-09.

[28] Z. Sun, C. Kasbergen, K.N. van Dalen, K. Anupam, A. Skarpas, S.M.J.G. Erkens, A parameter identification technique for traffic speed deflectometer tests of pavements, Road. Mater. Pavement Des. vol. 24 (4) (2023) 1065–1087, https://doi.org/10.1080/14680629.2022.2060125.

[29] IRC:37–2018, Guidelines for the design of flexible pavements (Fourth Revision), New Delhi, Nov. 2018.

[30] IS:2720 - Part 40, Determination of free swell index of soils. India, 1997.

[31] Preethi Shailaja, Ranjitha Tangadagi, Manjunath Maddikeari, Bharath Ashwath, Sustainable effect of chemically treated aggregates on bond strength of bitumen, J. Green. Eng. vol. 10 (9) (2020) 5076–5089.

[32] B. of Indian Standards, IS 2386–1 (1963): Methods of Test for Aggregates for Concrete, Part I: Particle Size and Shape.

[33] B. of Indian Standards, IS 2386–4 (1963): Methods of test for aggregates for concrete, Part 4: Mechanical properties.

[34] ASTM: D6373, Standard Specification for Performance-Graded Asphalt Binder, West Conshohocken.

[35] IS: 1203–2022, Methods for Testing Tar and Bituminous Materials — Determination of Penetration. India, 2022, pp. 1–10.

[36] IS:1206 (Part 2), Methods for Testing Tar and Bituminous Materials — Determination of Viscosity. India, 2022, pp. 1–12.

[37] IS:1205–2022, Methods for Testing Tar and Bituminous Materials — Determination of Softening Point — Ring and Ball Apparatus. India, 2022, pp. 1–10.

[38] Asphalt Institute, MS-2: Asphalt mix design methods, 7th ed. Asphalt Institute, 2014.

[39] Y. Zhao, Y. Ni, W. Zeng, A consistent approach for characterising asphalt concrete based on generalised Maxwell or Kelvin model, Road. Mater. Pavement Des. vol. 15 (3) (2014) 674–690, https://doi.org/10.1080/14680629.2014.889030.

[40] N.W. Tschoegl, The phenomenological theory of linear viscoelastic behavior: an introduction, Springer, Science & Business Media, 2012.

[41] S.K. Srirangam, *Numerical simulation of tyre pavement interaction*, vol. 53, no. 9. 2013.

[42] Samer W. Katicha, Analysis of Hot Mix Asphalt (HMA) Linear Viscoelastic and Bimodular Properties Using Uniaxial Compression and Indirect Tension (IDT) Tests, Virginia Polytechnic Institute and State University, Blacksburg, Virginia, 2007.

[43] Y.R. Kim, J.S. Daniel, and H. Wen, Fatigue performance evaluation of WesTrack asphalt mixtures using viscoelastic continuum damage approach, Apr. 2002.

[44] A. [Schapery and \ S[W[Park, Methods of interconversion between linear viscoelastic material functions[Part II*an approximate analytical method.

[45] B. Sukumaran *et al.*, THREE DIMENSIONAL FINITE ELEMENT MODELING OF FLEXIBLE PAVEMENTS, 2004.

[46] B. Sukumaran, M. Willis, and N. Chamala, Three Dimensional Finite Element Modeling of Flexible Pavements, 2005.

[47] I.L. Howard, M. Asce, and K.A. Warren, Finite-Element Modeling of Instrumented Flexible Pavements under Stationary Transient Loading, doi: 10.1061/ASCE0733–947×2009135:253.

[48] Y.-H. Cho, B.F. Mccullough, and J. Weissmann, Considerations on Finite-Element Method Application in Pavement Structural Analysis.

[49] B. Sam Helwany, J. Dyer, and J. Leidy, FINITE-ELEMENT ANALYSES OF FLEXIBLE PAVEMENTS.

[50] Rahman M.T., Mahmud K., and Ahsan S., StressStrain characteristics of flexible pavement using Finite Element Analysis, 2011.

[51] M.N.S. Hadi, B.C. Bodhinayake, Non-linear finite element analysis of flexible pavements. in Advances in Engineering Software, Elsevier Ltd, 2003, pp. 657–662, https://doi.org/10.1016/S0965-9978(03)00109-1.

[52] J.M. Duncan, C.L. Monismith, and E.L. Wilson, Finite Element Analyses of Pavements.

[53] F. Tang, T. Ma, Y. Guan, Z. Zhang, Parametric modeling and structure verification of asphalt pavement based on BIM-ABAQUS, Autom. Constr. vol. 111 (2020), https://doi.org/10.1016/j.autcon.2019.103066.

[54] P. Liu, Q. Xing, Y. Dong, D. Wang, M. Oeser, S. Yuan, Application of Finite Layer Method in Pavement Structural Analysis, Appl. Sci. vol. 7 (6) (2017) 611, https://doi.org/10.3390/app7060611.
[55] E. Parente Junior, J.B. Soares, Á. Silva de Holanda, E. Parente Junior Teresa Denyse Pereira de Araújo, and L. Tadeu Barroso de Melo Francisco Evangelista Junior Jorge Barbosa Soares, FINITE ELEMENT MODELING OF FLEXIBLE PAVEMENTS, 2006. [Online]. Available: https://www.researchgate.net/publication/281974814.
[56] Y.H. Huang. Pavement analysis and design, Second ed., Pearson Prentice Hall, Upper Saddle River, NJ, 1993.
[57] AASHTO: T 322-03, Determining the Creep Compliance and Strength of Hot-Mix Asphalt (HMA) Using the Indirect Tensile Test Device, American Association of State Highway and Transportation Officials, Washington D.C., USA, 2005, pp. 1–11.
[58] K. Anupam, T. Tang, C. Kasbergen, A. Scarpas, S. Erkens, 3-D thermomechanical tire–pavement interaction model for evaluation of pavement skid resistance, Transp. Res Rec. vol. 2675 (3) (2020) 65–80, https://doi.org/10.1177/0361198120963101.